

Purdue University

Purdue e-Pubs

International Refrigeration and Air Conditioning
Conference

School of Mechanical Engineering

2022

Load-based Testing of Heating and Cooling Equipment Informed by Detailed Energy Models

Aleksandr Fridlyand

Alejandro Baez Guada

Navin Kumar

Abbas Ahsan

Tim Kingston

See next page for additional authors

Follow this and additional works at: <https://docs.lib.purdue.edu/iracc>

Fridlyand, Aleksandr; Baez Guada, Alejandro; Kumar, Navin; Ahsan, Abbas; Kingston, Tim; and Glanville, Paul, "Load-based Testing of Heating and Cooling Equipment Informed by Detailed Energy Models" (2022). *International Refrigeration and Air Conditioning Conference*. Paper 2390.
<https://docs.lib.purdue.edu/iracc/2390>

This document has been made available through Purdue e-Pubs, a service of the Purdue University Libraries. Please contact epubs@purdue.edu for additional information. Complete proceedings may be acquired in print and on CD-ROM directly from the Ray W. Herrick Laboratories at <https://engineering.purdue.edu/Herrick/Events/orderlit.html>

Authors

Aleksandr Fridlyand, Alejandro Baez Guada, Navin Kumar, Abbas Ahsan, Tim Kingston, and Paul Glanville

Load-based Testing of Heating and Cooling Equipment Informed by Detailed Energy Models

Aleksandr FRIDLYAND^{1*}, Alejandro Baez GUADA¹, Navin KUMAR¹, Abbas AHSAN¹, Tim KINGSTON¹, Paul GLANVILLE¹

¹GTI Energy, Building Energy Efficiency
Des Plaines, IL, USA
(+1-847-768-0500; afridlyand@gti.energy)

* Corresponding Author

ABSTRACT

Load-based testing is an emerging approach for evaluating and rating heating and cooling equipment by simulating the transient nature of loads in the lab to emulate real world operating conditions as closely as possible. These test methods aim to generate more accurate performance data (e.g., coefficient of performance) that can be translated into useful ratings to compare disparate equipment, as well as performance maps that can be directly used with building energy modeling software. There are several industry and academic efforts to develop these procedures such that they may someday replace existing methods of testing and rating HVAC&R equipment.

One of the approaches for load-based tests is to couple the laboratory equipment to detailed building energy modeling software in a “Hardware-in-the-Loop” type system. The building energy models accept integrated energy input and output from the tested equipment and output information about the building’s thermal response (e.g., indoor air temperature change) This information is then used to control the return air/water conditions and/or to simulate thermostat calls. This type of approach can be complex but potentially offers the most accurate representation of real loads. Reduced order building models offer a much simpler approach for integration but are challenged by very rough approximations of the building and loads. In this paper, a hybrid approach is presented that uses a lumped heat capacitance approach for load-based testing in the lab but informs the necessary parameters from detailed building energy simulations. This approach was applied to evaluating part-load operation of a condensing modulating furnace operated under different control strategies, with results presented in this paper. The features, benefits, as well as limitations of this approach are also discussed.

1. INTRODUCTION

In 2022, buildings in North America are projected to consume approximately 35 EJ of primary energy while emitting 1420 metric tons of CO₂, of which approximately 60% can be attributed to space heating, space cooling, and water heating (Baseline Energy Calculator, 2022). To meet aggressive decarbonization objectives in the coming years and decades, existing buildings will need to undergo deep energy efficiency retrofits, energy supply to the buildings must be decarbonized, and to help close the gap, high efficiency heating and cooling appliances will need to be deployed. However, in many cases, the appliances being installed are lowest cost and/or minimum efficiency. If a building owner or a builder does want to install more efficient appliances, choosing the most energy efficient and/or cost-effective appliances can be challenging due to a plethora of standard efficiency ratings for different categories of appliances (e.g., Figure 1). In most cases, specific rating types are designed to enable comparison between similar appliances and not with those from different categories, making cross-product assessment of energy and cost savings difficult, especially when a fuel switch, hybrid, and combined systems are considered. For instance, if someone would like to compare different space heating options for a residential building, they could be faced with incompatible ratings from these example rating methods:

1. Warm air furnaces and boilers (ASHRAE 103 - Method Of Testing For Annual Fuel Utilization Efficiency Of Residential Central Furnaces And Boilers)
2. Electric heat pumps (AHRI 210/240 - Performance Rating of Unitary Air-conditioning & Air-source Heat Pump Equipment)

3. Tankless water heater based combined space and water heating systems (ASHRAE 124 – Methods of Testing for Rating Combination Space-Heating and Water-Heating Appliances or CAN/CSA-P.9-11 R2020 Test Method for Determining the Performance of Combined Space and Water Heating Systems (Combos))
4. Fuel-fired Heat Pumps (ANSI Z21.40.4 – Performance Testing And Rating Of Gas-Fired, Air Conditioning And Heat Pump Appliances)

All of these and other methods of testing and rating equipment seek to provide similar information (e.g., characteristic seasonal performance, annual energy consumption), but how they do it differs substantially. For some appliance categories, there are no standard methods of testing and rating (e.g., ground-source heat pumps, hybrid heat pumps), making comparisons impossible. More challenging yet, even within specific product categories, the existing product ratings will provide inaccurate comparisons between comparable products (Bruce Harley Energy Consulting LLC, 2020) (Baez Guada & Kingston, 2022) or poor predictions of actual seasonal performance (Fairey et al, 2004) (Bohac et al, 2010) (Fridlyand, et al, 2021) (Baez Guada & Kingston, 2022).



Figure 1. Examples of residential forced-air heating appliances rated to three different standards: Fuel-fired Heat Pumps – ANSI Z21.40.4 (L), Furnaces – ASHRAE 103 (M), Electric Heat Pumps – AHRI 210/240 (R)

One approach to overcome the shortcomings of predicting annual energy performance by standard equipment ratings is to perform field demonstrations where baseline and alternative equipment can be compared in actual usage. Significant limitations of this approach are that it is lengthy, requires a large sample size for accurate comparison, expensive, and fraught with uncertainties due to poor reproducibility attributed to environmental, human, and regulatory factors, e.g., Kingston et al (2016). Another solution to make up for existing rating method deficiencies is to use building energy simulations with detailed performance maps of equipment to quantify their impact of energy usage in various building and climate scenarios as well as to compare dissimilar equipment, e.g., Fridlyand & Liszka (2019) and Fridlyand et al (2021). However, the performance maps that are needed to run these simulations are frequently more comprehensive than the data collected and reported as part of standard methods of testing, therefore requiring additional testing, e.g., Fridlyand & Liszka (2019) and Baez Guada & Kingston (2022). Many of these problems could be overcome if the methods of testing and rating could generate compatible ratings across product categories and/or provide sufficient performance data to enable accurate building energy simulations without additional testing.

A potential unified solution is to implement “simulated use” or “load-based testing” procedures. In this approach, a real appliance under test is coupled to a detailed virtual building model such that the building model runs in real time and imposes heating (or cooling) loads using simulated thermostat calls and domestic hot water draws using electronically-actuated valves. When the equipment operates, under its native controls, the integrated heating (or cooling) energy is fed back into the building energy simulation which then uses the information to predict the indoor air temperature, e.g., Pratt et al (2017). Frequently referred to as “Hardware-in-the-Loop” (HIL) testing, this approach potentially permits the testing of complicated interactions in integrated energy system (e.g., power generation, controls, as well as HVAC equipment). In the ideal scenario, HIL testing permits close replication of real-world conditions, but in a far more controlled environment. However, as a practical approach for testing and rating appliances, using detailed building energy models has limitations. The building energy simulations can be complex, requiring the coupling of multiple software stacks and fast computers. HIL simulations may also require additional consideration of “warm-up” procedures of the building to have a repeatable test. Since the building model runs in real

time, including the simulation of outdoor conditions, it may require hours or days of testing to achieve reproducible conditions. These complications make load-based testing with detailed building energy models impractical as a standard method of testing and rating equipment.

An alternative approach for testing equipment under simulated use conditions is to use reduced order models (ROM) of the building. This is currently one of the leading approaches being developed for load-based testing and rating methods in North America, such as its implementation in the CSA EXP07 test method (Bruce Harley Energy Consulting LLC, 2020) and recent development by researchers from Purdue University (Patil et al, 2018), (Dhillon et al, 2018). In this approach, ROMs are used to simulate the interaction of a building's thermal envelope with the outdoor conditions and the heating/cooling provided by the appliance. The ROM used in CSA EXP07 is based on a lumped heat capacitance (LHC) approach, where the entirety of the building's thermal mass is reduced to a single value C [J/°C], representing the energy required to raise the temperature (equated to that of average air-temperature) of the building by one degree. The room temperature T_R [°C] can then be predicted using the following equation:

$$T_R(t + \Delta t) = T_R(t) + \frac{\Delta t(BL - \dot{Q}_s)}{C} \quad (1)$$

Where T_R is the room temperature at a specific time t [s], Δt [W] is the time step of integration, BL [W] is the building load (a function of outdoor temperature) and \dot{Q}_s [W] is the heating/cooling rate provided by the equipment under test over period of Δt . In the CSA EXP07 method of test, both BL and C are defined in terms of the steady state capacities of the equipment under test at reference outdoor conditions (e.g., cooling capacity at 35°C outdoor dry bulb temperature). The potential limitation of this approach is that the exact test conditions are specific to the equipment. The loads, the capacitance, and therefore things like modulation rate and cycling frequency are equipment specific in CSA EXP07, potentially limiting the method's usefulness in enabling comparison between different types of equipment (not a stated objective of CSA EXP07). It is also not clear whether the data being collected is characteristic of real world-conditions as the model parameters are not related to any specific building type. To elaborate, one building with a low thermal mass and another with a high thermal mass may have the same design loads and would therefore be sized for the same capacity equipment. However, the building with the lower thermal mass will experience more rapid changes in temperatures and could force the equipment to cycle more frequently than a building with a high thermal mass.

This paper describes an alternative approach that is like the LHC method used in CSA EXP07 but calibrates the capacitance based on detailed building energy simulations. In doing so, the performance of disparate equipment can be compared using the same load conditions. The remainder of the paper describes model formulation and calibration approach using detailed building energy simulations, assessment of the approach using a modulating, condensing furnace, as well as a discussion of the features, limitations, and potential future steps with the new test method.

2. MODEL DEVELOPMENT AND CALIBRATION

The load-based test method implemented in this study is like that developed for CSA EXP07 where the time-dependent temperature of the building can be approximated by Eq.1. A quick examination of the equation's form makes apparent that the model behaves in a manner expected of a conditioned building:

1. If the building load and heating/cooling supplied are balanced, the temperature does not change
2. If the building load is greater or smaller than the heating/cooling supplied, the temperature will change at a rate equal to the third term in Eq.1.

The inputs into this model are the initial temperature, building load, and the lumped capacitance. Figure 2 (L) plots the predicted LHC temperature change using Eq.1 for a case where the building starts at 21°C and experience gradual cooling due to heat loss at various outdoor temperature. For comparison, Figure 2 (R) plots the LHC temperature change where a thermostat attempts to control the temperature to 21°C with a 0.6°C dead band, using a simple constant capacity heating device (e.g., a furnace).

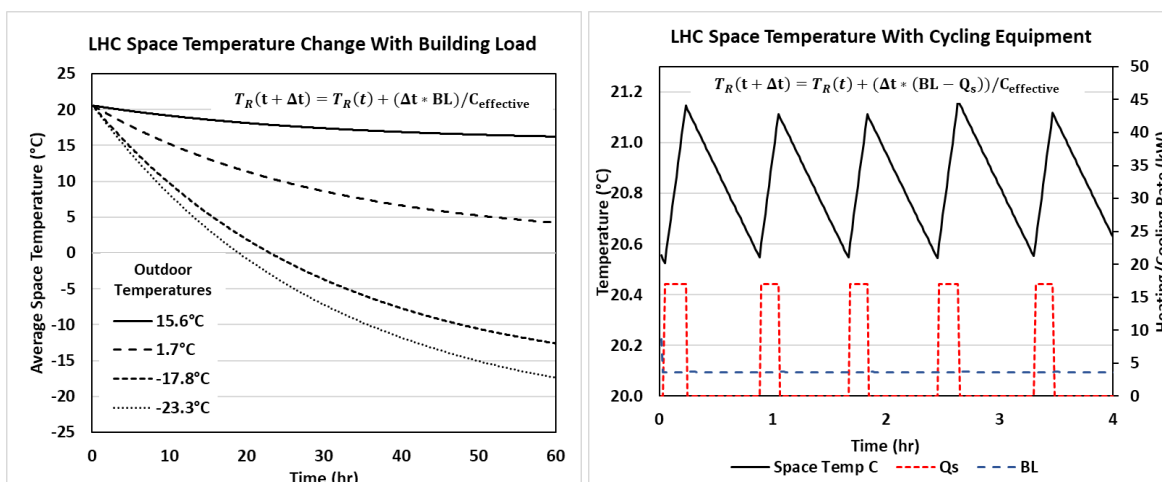


Figure 2. Predicted temperature change due to heat loss from a building using Eq.1, starting temperature of 21°C (L) The same case but with a thermostat controlling the LHC temperature to 21°C with a 0.6°C dead band (R). In both cases, the $C_{effective}$ is 14.2 MJ/°C and $BL = UA(T - T_{outdoor})$, with $UA = 132 \text{ W/°C}$.

The main difference between the CSA EXP07 method and the present study is that it uses a lumped heat capacitance that is a function of the cooling capacity of the equipment, while here the effective lumped capacitance of a representative building is used. Antonopoulos and Koronaki (1998) make a distinction between “apparent” and “effective” thermal capacitance. Apparent building capacitance is equal to the sum of individual capacitances of the building materials of construction, furniture, air, and anything else inside the envelope that can store thermal energy. In contrast, the effective capacitance of a building is a value of C that minimizes the error between the predictions of Eq. 1 and the temperature-time history of the thermal zone inside a building. They showed that apparent and effective capacitances of a building are not the same, with the former shown to be 2-3 times greater than the latter. The effective capacitance can be determined from least squares fit of Eq. 1 to temperature-time history data such as shown in Figure 2 (L) if the load of the building is known. In the work of Antonopoulos and Koronaki, the authors determined the effective capacitance by using data from more detailed building energy simulations.

The advantages of using Eq. 1 and an effective building capacitance are its simplicity, ease with which it can be solved, and when coupled with a simple thermostat simulator, can be used to predict either thermostat calls and/or the room/return air temperature. One limitation of this approach is that the effective thermal capacitance is not constant and instead depends on indoor and outdoor conditions (as will be shown later). Another limitation is that it cannot predict very rapid changes in indoor temperature if the building is subjected to rapidly changing loads. However, it is not the purpose of the present study to perform accurate building energy simulations but to reproduce more realistic test conditions for which it has been shown that the LHC approach is adequate (Dhillon et al, 2018) (Patil et al, 2018) (Bruce Harley Energy Consulting LLC, 2020).

To use the LHC model in a load-based test method to compare different types of equipment, the model in the present study was first calibrated against detailed building energy simulations using EnergyPlus 8.8 and BEopt (2.8). A detailed model of single-family home was first constructed using BEopt that is approximately 280 m² with an ~IECC 2012 building envelope, 4-bedrooms, 3-baths, two-car attached garage, and a heated-unfinished basement. In the ASHRAE Climate Zone 5A (Chicago, IL, USA), this building has a design heating load of 10 kW. The model was originally developed to assess the seasonal performance of a nominally 12 kW gas absorption heat pump, similar to the system described by some of the authors previously (Fridlyand et al, 2021). Because effective capacitance is not one of the standard outputs from BEopt, it had to be inferred from EnergyPlus simulations using a custom weather file, availability schedules, and equipment controls.

The custom weather file removed solar radiation, wind, and set a constant outdoor temperature and humidity for a heating or cooling month. The building was then simulated for four to five days, with the first few days the HVAC equipment (central furnace and an A/C) operating normally. The initial days were used to make sure the building was under a steady load and to determine the heating and cooling loads as a function of outdoor and indoor temperatures (taken to be the heating or cooling delivered by the HVAC equipment). On the last day, the HVAC equipment was

turned off and the building allowed to cool down or heat up, depending on the season. The temperature-time history data from these simulations was then used with Eq. 1 to infer the effective thermal capacitance. Examples of these simulations and the resulting fit of Eq. 1 are shown in Figure 3.

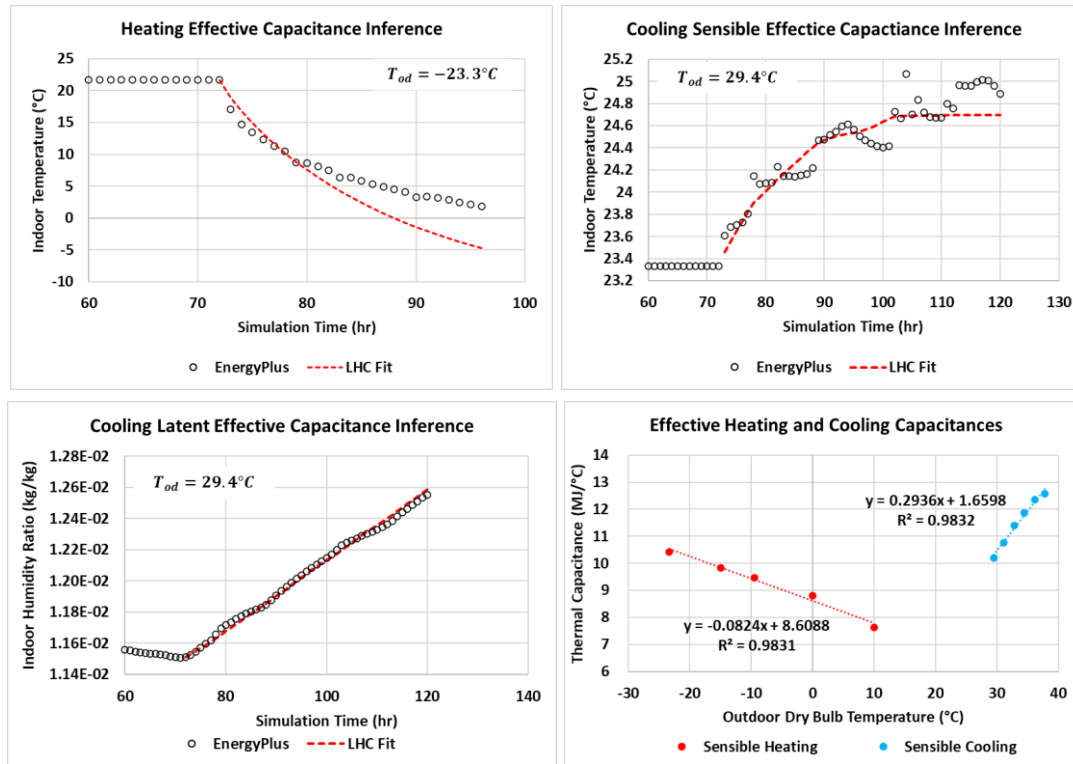


Figure 3. Example Temperature-time history used for inference of heating effective capacitance (TL), sensible cooling capacitance (TR), humidity-time history for latent cooling (BL) and the resulting relationships for sensible heating and cooling capacitances as a function of outdoor dry bulb temperature (BR).

In addition to the sensible capacitance for heating and cooling in Figure 3, the figure also plots the results of fitting the latent effective capacitance, or the “moisture capacitance” (Patil et al, 2018), which allows the moisture dynamics of the building to be modeled in a simplified way as well using Eq. 2:

$$w(t + \Delta t) = w(t) + \frac{\Delta t(LL + \dot{Q}_l)}{h_{fg}C_w} \quad (2)$$

Where w is the space humidity ratio [kg/kg], LL is the space latent cooling load [W], \dot{Q}_l is the latent cooling provided by the HVAC equipment [W], h_{fg} is the enthalpy of vaporization [J/kg], and C_w is the moisture capacitance [kg]. Unlike the sensible capacitances, the moisture capacitance was not a strong function of outdoor and indoor humidity and was therefore taken to be an average of all simulations 16,285 kg. While not discussed further in this paper (to be further presented in a future publication), the determination of the moisture capacitance is included here for completeness to demonstrate that it can also be obtained from the detailed building energy simulations.

Except for the moisture capacitance fit, both the sensible heating and cooling capacitances in Figure 3 show imperfect fits to the temperature-time profiles. The non-smooth behavior of the temperature from detailed simulations is due to intermittent indoor loads, which operated on schedules that were not modified for these simulations. The effect is more pronounced for the 29.4°C cooling simulations because the exterior cooling load was the lowest compared to indoor sensible loads. On the warmest day of 38°C, the temperature history was smoother, like the heating example plotted in Figure 3 at -23.3°C, which was the coldest day. Initial regression fits of Eq. 1 to the detailed simulation data did not produce a satisfactory fit over the full temperature-time history. However, since the purpose of the LHC model is to capture the short duration temperature changes when the equipment cycles on and off, the regression was reformulated to only fit the first two hours of the cooling/heating period, resulting in the fits plotted in Figure 3. This does show one of the limitations of the LHC model is that it may not be able to accurately capture large/rapid temperature swings, e.g., large temperature setback recoveries.

For comparison of magnitudes, a heating thermal capacitance was estimated for the home of one of the authors from smart thermostat data for a cycling gas furnace of 23.4 kW heating capacity that was observed to cycle at a steady frequency during a 0°C day in April in Chicago, equating to a part load ratio (PLR = load/capacity) of ~15%. With a constant setpoint of 21.7°C and a 0.6°C dead band, the furnace was observed to cycle-on five times in a 4-hour period. To reproduce the same behavior using the simple LHC + thermostat model in Figure 2, the effective thermal capacitance was estimated to be 13.2 MJ/°C. The home served by this furnace was a 260 m² duplex-down condominium in a 6-unit building built in 2004. The effective capacitance for heating from the detailed building energy models in Figure 3 was 8-10.5 MJ/°C, indicating that the order of magnitude is correct. For both sensible heating and cooling, the effective capacitance was found to be a strong function of outdoor temperature for a fixed indoor setpoint. This is contrary the findings of Antonopoulos and Koronaki (1998), who showed that the effective capacitance is constant based on their more limited building energy simulations.

3. EXPERIMENTAL EVALUATION

The LHC model described in Section 1 was implemented in a gas furnace test apparatus as a control program that integrates Eq. 1 in time given a steady or time-varying heating load and measured heat delivered from the furnace. A simple thermostat program simulated called for heat to maintain a constant setpoint of 21.7°C with a 0.6°C dead band. The test apparatus is schematically illustrated in Figure 4. It is described more in a prior publication (Baez Guada & Kingston, 2022), so only a brief description is provided here. The apparatus consists of an air flow measurement section (averaging pitot-static tubes - ±2% accuracy) and a conditioning section that connects to the air return of the furnace. Dry bulb temperature at the inlet and outlet of the furnace are collected using 9-point arrays of T-type thermocouples (±1°C), while the moisture content was measured using a relative humidity transmitter (±2% accuracy). Using the air flow and psychrometric measurements an air-side energy balance was performed to continuously monitor the heat output of the unit. Measured and integrated every five seconds, the heat delivered was used as input into an LHC program which would calculate a new “room temperature” for the next five seconds. In a full integrated approach, this room temperature becomes the target setpoint for the conditioning coils upstream of the furnace. In the present study, the return air was not conditioned and varied with ambient lab temperature (18.3 – 23.9°C). This had the effect of introducing a small variability to the measured efficiencies discussed later. To complete the energy balance in this study, gas consumption was measured using a totalizing diaphragm gas meter (±1% accuracy). The heating value at standard conditions was determined using gas chromatography and calculated based on composition and then adjusted to local temperature and pressure conditions.

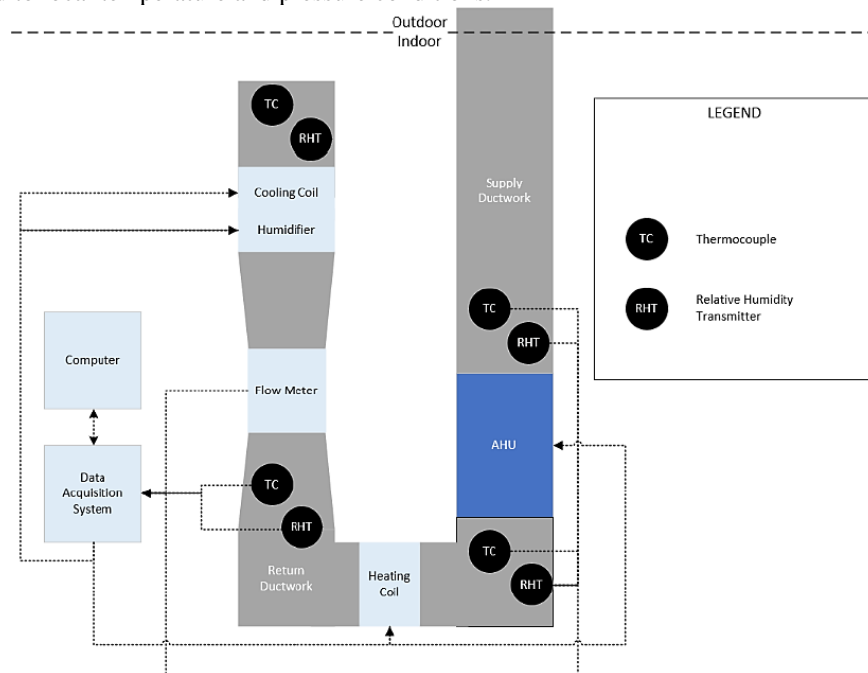


Figure 4. Furnace test apparatus used in the present investigation, described in more detail in a prior publication by the authors (Baez Guada & Kingston, 2022)

In parallel to the LHC program that updated the room temperature, a simple thermostat program was implemented that would either cycle the equipment on and off at a single speed within a 0.6°C dead band or the thermostat program could send a pulse-width modulation signal proportional to the room temperature within the dead band. The furnace tested was a commercially available, 17 kW rated output condensing unit (AFUE > 95) that could operate in either single-stage cycling mode or modulate between 40% and 100%. This furnace was tested in both configurations at three different load levels, described in Table 1. The effective capacitance and the heating loads were scaled by 33% to better match the furnace tested because the capacitances inferred in Section 2 were for a lower-load home for which this furnace would be significantly oversized. Figure 5 plots representative time profiles of the heat delivered, gas used, the virtual room temperature T_R .

Load Level	Effective Capacitance (MJ/°C)	Heating Load (kW)	PLR
1	14.1	10.2	60%
2	12.0	5.2	30%
3	10.6	2.3	14%

Table 1. Heating load levels tested with the gas furnace under cycling and modulating controls

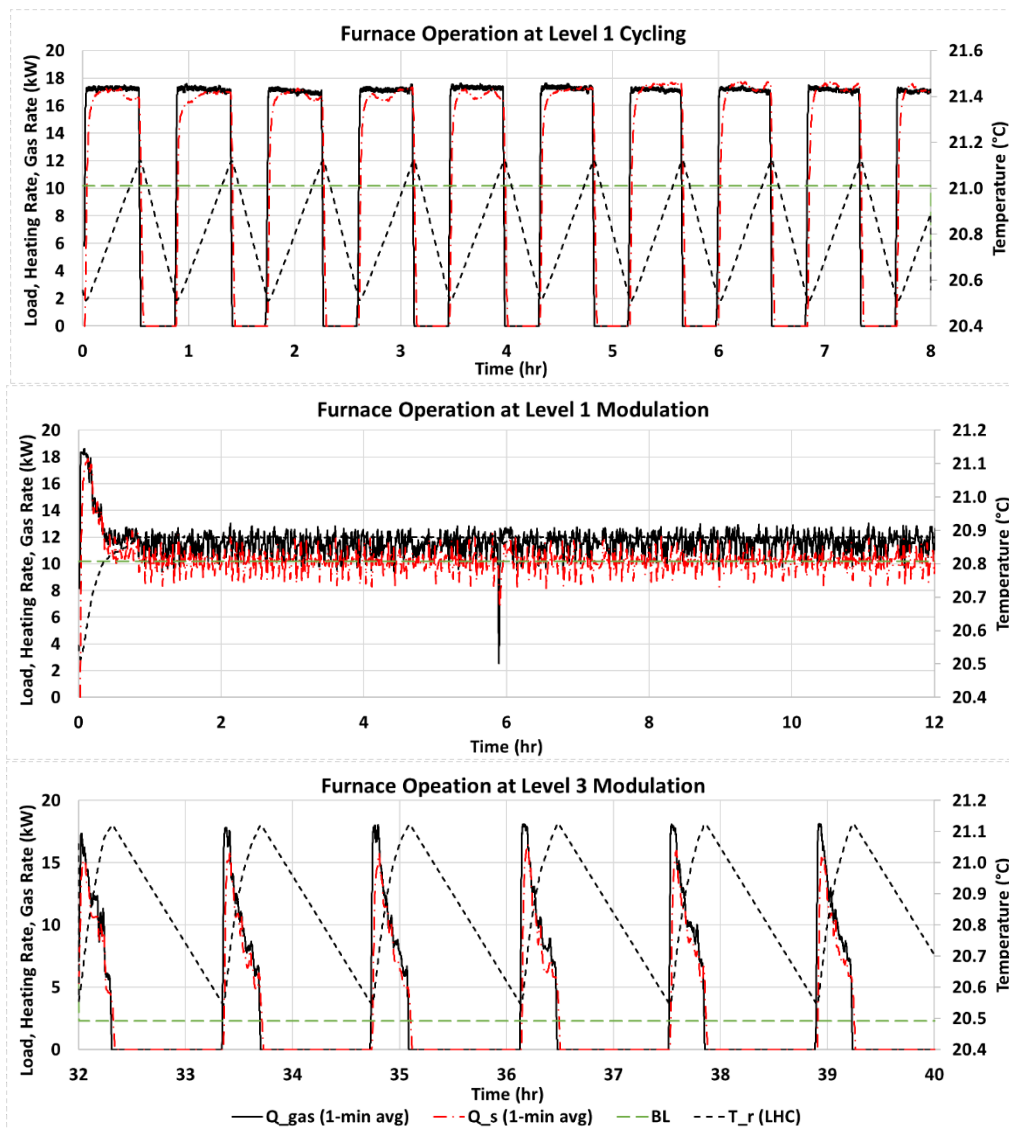


Figure 5. Temperature time-histories, load, heat delivered, and gas used during furnace single-stage cycling operation at load level 1 (T), modulation at load level 1 (M), and modulation at load level 3 (B)

The part-load tests at each level and control configuration were performed for varying lengths of time between 8 and 24 hours to ascertain duration needed to achieve repeatable results. At load level 3, the furnace would cycle as little as once an hour, so several hours were needed to verify repeatability. The tests were conducted with each load level run in sequence. The apparatus controls were reset at the end of the test level period and the furnace allowed to recover from $T_r = 20.6^\circ\text{C}$. Overall, after approximately 5 hours, the tests were repeatable at each condition, with some nuances described later. Qualitatively, the furnace and the LHC control program behaved as expected with cycling frequencies and on/off durations comparable to predictions (8-30 minute on-times and 17-70 minute off-times). Under load Level 1 and 2, the furnace was able to modulate continuously, while under load level 3, the furnace attempted to modulate but had to cycle off when the setpoint was reached (Figure 5 (B)). The furnace tested would modulate in discrete steps, which is most evident in the level 3 modulation tests.

To assess the repeatability of the test and furnace behavior, the gas efficiency was calculated as a ratio of heat delivered to gas used either over a fixed duration or a complete on-off cycle, taken to be from midpoint to midpoint of the off periods. Figure 6 plots the two-hour window average gas efficiency for the modulating tests as well as the cycle-averaged efficiency for the level 3 modulation test. For all three modulation cases, following an initially elevated efficiency due to a reset in controls and a recovery, the furnace settled into a repeatable pattern after five hours, with minor fluctuations except at level 3 modulation. The level 3 modulation test was run for 24 hours, and during an 8-hour period the lab temperatures dropped from $\sim 23.8^\circ\text{C}$ to 18.3°C , which was the only variable that correlated with the rise in efficiency seen around cycle 9. As noted earlier, in more integrated tests, the return-air temperature to the equipment being tested should be tied to the predicted T_R from the Eq. 1. What is most notable in the modulating tests are that in all cases the gas efficiency falls short of AFUE ($>95\%$). The reason for this is best explained with comparison to the single-stage cycling tests.

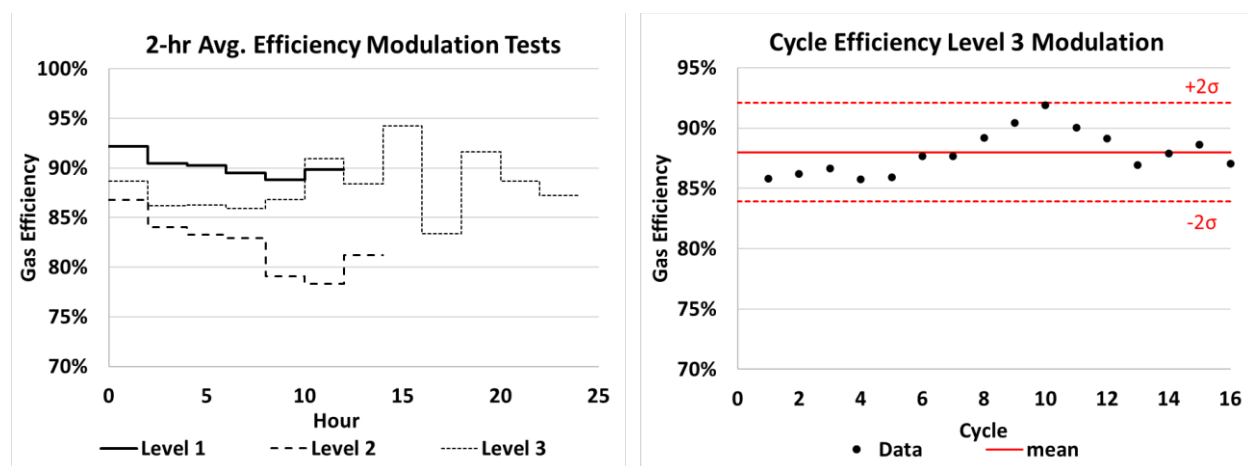


Figure 6. Two-hour window gas efficiency for the modulation tests (L) and cycle-average efficiency for level 3 modulation test (R)

Figure 7 (L) plots the cycle-average efficiencies from the single-stage cycling tests, where the furnace was fired at 100% until the thermostat program was satisfied and then turned off until the temperature fell below the dead band. At all three test levels, the average gas efficiency was greater than 90%, with Level 1 tests averaging $>95\%$ efficiency. Figure 7 (R) compares the cumulative tests results between the modulation and single-stage cycling tests as a function of PLR. This plot shows a consistent trend of modulating performance being 5-10% lower than single-stage cycling tests. This is counterintuitive at first, however the controls specific to this furnace explain the difference. While the furnace gas valve and system blower have several stages for modulation, the inducer blower on the combustion system, only has two. The furnace is tuned to optimally operate at 100% firing rate, where its O_2 concentration in the flue gases is $\sim 8\%$ (dry basis). However, at low modulation level, the O_2 level rises to $\sim 15\%$. This is a difference of $\sim 55\%$ excess air at maximum firing rate and $\sim 250\%$ excess air at low modulation levels, meaning that the hot flue-gases are more dilute when modulating, reducing the potential for heat that can be captured. This trend also explains why the 14% load level modulation tests resulted in a higher efficiency. When cycling-on and off, the furnace started operation at maximum fire and then modulated down as the room temperature increased. For the modulation tests, the furnace spent more time at higher modulation levels than at level 2, yielding a higher gas efficiency. A more optimal control strategy would be to have more stages on the inducer to keep the O_2 level constant, in which case the efficiency may be higher at lower modulation levels where the heat exchanger would be oversized. Given that the rated AFUE of this

furnace is >95%, this reduced-performance while modulating is not correctly captured by this metric, showing its deficiency.

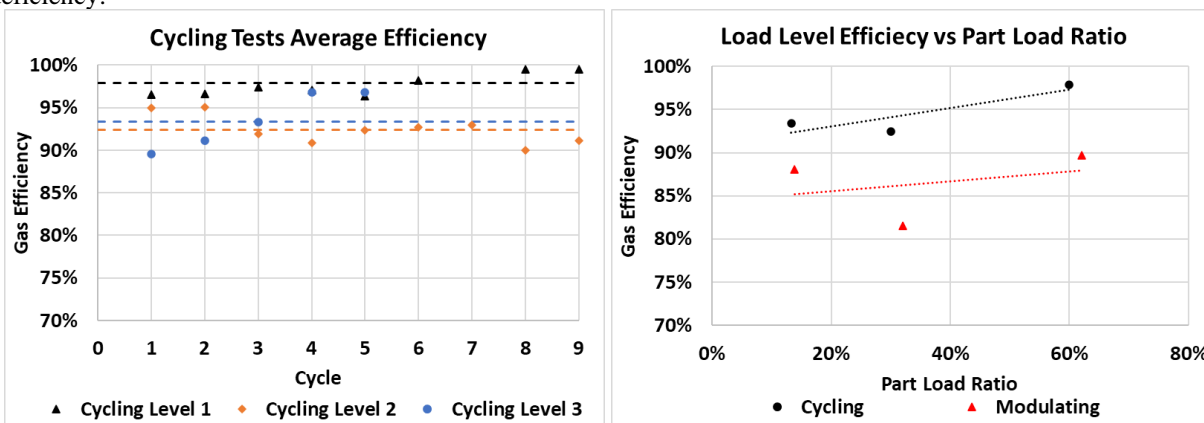


Figure 7. Cycle-average gas efficiency for the cycling tests (L) and total gas efficiency for each test level (R)

4. DISCUSSION AND CONCLUSIONS

This study presented a modification of the Lumped Heat Capacitance (LHC) approach for performing load-based tests that was previously developed for testing heat pumps and air conditioners under CSA EXP07. The objective of the modifications was to develop a more generalized LHC test method where the capacitance is taken to be the effective capacitance of a building, determined from detailed building energy simulations. Using this approach, disparate types of equipment can be tested and compared using the same methods, something that is not possible with existing approaches for testing and rating equipment such as heat pumps, furnaces, and hybrid systems.

The modified LHC load-based test was then evaluated by testing a condensing, modulating gas furnace under two different control strategies, single-stage cycling and modulation. The tests were performed at three different part-load levels (14-60%), while measuring the heat output and gas consumption during 8–24-hour tests. The tests of the load-based control algorithm yielded expected results with respect to cycling and modulation behavior but an unexpected trend with gas efficiency. For all modulation levels, the gas efficiency was 5-10% lower than for single-stage cycling tests. The reason for this trend was sub-optimal control of the flue gas dilution, a phenomenon not currently captured by the AFUE rating method.

Overall, this study demonstrates how the LHC load-based method can be effectively applied to different categories of equipment and reveal information about equipment that current test and rating methods are not able to. If deployed more broadly, this approach to testing and rating equipment could permit any product that provides the same service (e.g., warm air) to be compared, something not otherwise possible now. An environmental chamber for communicating thermostats would also permit testing under fully native controls (Cheng et al, 2021). Further expansions into a true “virtual test home” can overlay domestic hot water draws to test combined space and water heating systems and power generation equipment and electric loads for measuring the energy consumption of integrated energy systems. More elaboration on how to integrate multiple test protocols in an integrated test approach are provided elsewhere by some of the authors of this paper. (Baez Guada & Kingston, 2022). If this method is further developed into a standardized procedure for all equipment, it could beneficially lead to technology innovations because previously isolated product categories would compete directly.

REFERENCES

- Antonopoulos, K., & Koronaki, E. (1998). Apparent and Effective Thermal Capacitances of Buildings. *Energy*, 23(3), 183-192.
- Baez Guada, A., & Kingston, T. (2022). A Novel Approach to Determining As-installed Space and Water Heating Equipment Performance and Quantifying Potential Energy and Cost Savings in Buildings. *ASHRAE Transactions*, 128(1), LV-22-C021.

- Baez Guada, A., & Kingston, T. (2022). Combined Cold-climate Air-source Heat Pump and Heat Pump Water Heater System Performance in Multiple Climate Zones. *ASHRAE Transactions*, 128(1), LV-22-C019.
- Baseline Energy Calculator. (2022). (US DOE) Retrieved 3 2022, from <https://scout.energy.gov/baseline-energy-calculator.html>
- Bohac, D., Schoenbauer, B., Hewett, M., Lobenstein, M., & Butcher, T. (2010). Actual Savings and Performance of Natural Gas Tankless Water Heaters. Minnesota Office of Energy Security.
- Bruce Harley Energy Consulting LLC. (2020). EXP07:19 Load-based and Climate-Specific Testing and Rating Procedures for Heat Pumps and Air Conditioners: Interim Lab Testing and Rating Results REPORT #E20-314. NEEA. Retrieved from <https://neea.org/resources/exp0719-load-based-and-climate-specific-testing-and-rating-procedures-for-heat-pumps-and-air-conditioners>
- Building Energy Optimization (BEopt) 2.8 - <https://beopt.nrel.gov/>. (n.d.).
- Cheng, L., Braun, J. E., & Horton, W. T. (2021). Load-based Testing Using a Thermostat Environment Emulator. *International Journal of Refrigeration-revue Internationale Du Froid*, 126, 109-122.
- Dhillon, P., Patil, A., Cheng, L., Braun, J. E., & Horton, W. T. (2018). Performance Evaluation of Heat Pump Systems Based on a Load-based Testing Methodology. *International Refrigeration and Air Conditioning Conference*, Paper 2077. Retrieved from <https://docs.lib.purdue.edu/iracc/2077>
- EnergyPlus 8.8 - energyplus.net. (2018). DOE.
- Fairey, P., Parker, D., Wilcox, B., & Lombardi, M. (2004). Climate Impacts on Heating Seasonal Performance Factor (HSPF) and Seasonal Energy Efficiency Ratio (SEER) for Air Source Heat Pumps. *ASHRAE Transactions*, 110, 178.
- Fridlyand, A., & Liszka, M. (2019). Lab Testing of Tankless Water Heater Systems. NEEA. Retrieved from <https://neea.org/resources/lab-testing-of-tankless-water-heater-systems>
- Fridlyand, A., & Yuan, F. (2021). Non-Powered Damper Gas Storage Water Heater Lab Testing. NEEA. Retrieved from <https://neea.org/resources/non-powered-damper-gas-storage-water-heater-lab-testing>
- Fridlyand, A., Baez Guada, A., Kingston, T., & Glanville, P. (2021). Modeling Modern, Residential, Combined Space and Water Heating Systems Using EnergyPlus. *ASHRAE Transactions*, 127(1), 135-142.
- Fridlyand, A., Glanville, P., & Garrabrant, M. (2021). Pathways to Decarbonization of Residential Heating. *International High Performance Buildings Conference*, Paper 354. Retrieved from <https://docs.lib.purdue.edu/ihpbc/354>
- Fridlyand, A., Glanville, P., & Kumar, N. (2021). A Review and an Evaluation of the Updated Method of Test for Rating Fuel-fired Heat Pumps in HVAC. *ASHRAE Transactions*, LV-22-C024.
- Kingston, T., Vadnal, H., Scott, S., & Kalensky, D. (2016). Evaluation of Technical and Utility Programmatic Challenges With Residential Forced-Air Integrated Space/Water Heat Systems. United States: US DOE. doi:<https://doi.org/10.2172/1338438>
- Patil, A., Hjortland, A. J., Cheng, L., Dhillon, P., & Braun, J. E. (2018). Load-based testing to characterize the performance of variable-speed equipment. *International Refrigeration and Air Conditioning Conference*, Paper 2076. Retrieved from <https://docs.lib.purdue.edu/iracc/2076>
- Pratt, A., Ruth, M., Krishnamurthy, D., Sparn, B., Lunacek, M., Jones, W., . . . Marks, J. (2017). Hardware-in-the-loop simulation of a distribution system with air conditioners under model predictive control. 2017 IEEE Power & Energy Society General Meeting, 1-5. doi:10.1109/PESGM.2017.8273757

ACKNOWLEDGEMENT

The material presented in this paper is based upon work financially supported by Utilization Technology Development (NFP) under projects 1.16.H, 1.18.H, and 1.20.G.